

## Observations of surf beat forcing and dissipation

Stephen M. Henderson and A. J. Bowen

Department of Oceanography, Dalhousie University, Halifax, Nova Scotia, Canada

Received 15 June 2000; revised 14 August 2001; accepted 6 March 2002; published 13 November 2002.

[1] We used a simple energy balance equation, and estimates of the cross-shore energy flux carried by progressive surf beat, to calculate the rate of net surf beat forcing (or dissipation) on a beach near Duck, North Carolina. Far inside the surf zone, surf beat dissipation exceeded forcing. Outside the surf zone, surf beat forcing exceeded dissipation. When incident waves were large, surf beat dissipation inside the surf zone and forcing just outside the surf zone were both very strong (the surf beat energy dissipated in the surf zone in a single beat period was of the same order as the total amount of surf beat energy stored in the surf zone). During storms, shoreward propagation of surf beat maintained surf beat energy in the surf zone. Net surf beat dissipation in the surf zone scaled as predicted by a simple bottom stress parameterization. The inferred dissipation factor for surf beat was 0.08, within the range of wave dissipation factors usually observed in the field and 27–80 times larger than drag coefficients appropriate for the mean longshore current. The observed rapid forcing, rapid dissipation, and shoreward propagation of surf beat are not simulated by existing models of surf beat dynamics. *INDEX TERMS:* 4546 Oceanography: Physical: Nearshore processes; 4560 Oceanography: Physical: Surface waves and tides (1255); 3220 Mathematical Geophysics: Nonlinear dynamics; *KEYWORDS:* waves, infragravity, dissipation, nearshore, nonlinear

**Citation:** Henderson, S. M., and A. J. Bowen, Observations of surf beat forcing and dissipation, *J. Geophys. Res.*, 107(C11), 3193, doi:10.1029/2000JC000498, 2002.

### 1. Introduction

[2] In this paper we study the forcing and dissipation of low-frequency (0.005–0.05 Hz) gravity waves on a natural beach. These low-frequency gravity waves, often called infragravity waves or surf beat, are important in very shallow water where they often dominate water velocity and sea surface displacement fields [Guza and Thornton, 1982; Holman and Bowen, 1984]. Surf beat is generated primarily by nonlinear interactions with higher-frequency gravity waves [Munk, 1949; Longuet-Higgins and Stewart, 1962; Hasselmann et al., 1963; Symonds et al., 1982; Ruessink, 1998a].

[3] Surf beat dissipation is not understood. Several researchers have suggested mechanisms that could dissipate surf beat, including bottom friction [Guza and Davis, 1974; Lippmann et al., 1997], wave breaking [Bowen, 1977; Schäffer, 1993; Van Dongeren et al., 1996], and propagation of nonlinearly forced higher-frequency waves to deeper water [Guza and Bowen, 1976b; Mathew and Akylas, 1990]. Surf beat energy might also be lost from beaches by propagation of surf beat to deeper water [e.g., Schäffer, 1993; Chen and Guza, 1999]. These theories have not been tested against field observations and, because wave breaking is not fully understood, it is not known which of the possible dissipation mechanisms is most important.

[4] Two types of freely propagating surf beat exist: edge waves and leaky waves. Edge waves are trapped close to the shore by refraction, whereas leaky waves can propagate to and from deep water. If dissipation is sufficiently weak then edge and leaky waves respond to forcing in a strongly resonant manner and dominate surf beat. Bowen and Guza [1978] and others have suggested that edge waves might become larger than leaky waves because they are trapped in shallow water where nonlinear forcing is strong.

[5] If dissipation is strong then the effects of forcing can not accumulate over many wave periods, so resonance is suppressed and qualitatively new behavior is expected. The degree to which a free (leaky or edge wave) mode dominates over nonresonant modes is determined by the parameter [Green, 1955]

$$Q = 2\pi \frac{\text{Total energy of mode}}{\text{Energy of mode dissipated in a single wave period}} \quad (1)$$

Note that  $Q$  is approximately the timescale for wave dissipation divided by the wave period, so a low  $Q$  indicates rapid dissipation and a high  $Q$  indicates slow dissipation. Only if  $Q \gg 1$  can the effects of forcing accumulate over many wave periods, generating a strong resonant response.

[6] Most models of surf beat dynamics neglect dissipation [Eckart, 1951; Ursell, 1952; Kenyon, 1970; Holman and Bowen, 1979, 1982; Symonds, 1982; Mei and Benmoussa, 1984; Liu, 1989; Howd et al., 1992; List, 1992;

Bryan and Bowen, 1996; Schäffer, 1993, 1994] or assume that dissipation is asymptotically weak [Gallagher, 1971; Foda and Mei, 1981; Lippmann et al., 1997]. These high  $Q$  models successfully predict many features of the observed cross-shore [Huntley, 1976; Holland et al., 1995], longshore [Huntley et al., 1981; Oltman-Shay and Guza, 1987; Bryan et al., 1998], and frequency domain [Holman, 1981; Guza and Thornton, 1985] structure of surf beat. The success of high  $Q$  models suggests that the  $Q$  of surf beat is often high [Holman, 1981]. However, strong correlations are often observed between surf beat and local nonlinear forcing [Munk, 1949; Tucker, 1950; Huntley and Kim, 1984; Guza et al., 1984; List, 1986, 1992; Masselink, 1995; Ruessink, 1998a], suggesting that a significant amount of energy is carried by modes that are not resonantly forced ('forced modes'). Observations of strong correlations between surf beat and local nonlinear forcing lead Huntley and Kim [1984] to conclude that the low-frequency ( $<0.03\text{Hz}$ ) surf beat they observed was not dominated by free (i.e., high  $Q$ , resonantly forced) waves.

[7] Longuet-Higgins and Stewart [1962] showed that the strength of the response of surf beat to forcing increases with decreasing water depth. Symonds et al. [1982] suggested that a significant amount of surf beat forcing occurs at the edge of the surf zone, where wave breaking is intermittent, and no forcing occurs inside the saturated surf zone. Huntley and Kim [1984], List [1986], Masselink [1995], and Ruessink [1998a, 1998b] found that correlations between surf beat and nonlinear forcing increase with increasing wave height and decreasing water depth until intense wave breaking occurs, at which stage correlations suddenly decline. These observations are in qualitative agreement with the theories of Longuet-Higgins and Stewart [1962] and Symonds et al. [1982]; however, no quantitative relationship between the observed correlation strength and the strength of surf beat forcing near the shore has been derived. Farther offshore ( $\geq 8$  m water depth) only a small proportion of low-frequency energy can be explained by local nonlinear forcing, although this proportion does increase during storms [Okiihiro et al., 1992; Elgar et al., 1992; Herbers et al., 1994, 1995b]. Munk et al. [1964] found that strongly resonant (high  $Q$ ) edge waves dominated the infragravity energy they observed in 7 m water depth on the Californian Continental Shelf.

[8] Guza and Bowen [1976a], Bowen [1977], Bowen and Guza [1978], Huntley et al. [1981], and Bryan and Bowen [1996] suggested that wave breaking might lead to particularly strong surf beat dissipation inside the surf zone. Feddersen et al. [1998] showed that the bottom drag coefficient for the mean longshore current is about three times larger inside the surf zone than outside the surf zone. Observations of progressive infragravity waves [Elgar et al., 1994] and infragravity energy fluxes [Herbers et al., 1995a] in  $\geq 8$  m water depth suggest that infragravity waves can be significantly dissipated on the continental shelf during storms.

[9] The purpose of this paper is to determine the approximate strength and cross-shore structure of surf beat forcing and dissipation. In section 2 we present a simple energy balance equation for surf beat. We show that this energy balance equation can be combined with measurements of water pressure, velocity, and depth to yield spatially aver-

aged rates of net surf beat forcing (or dissipation). This method provides estimates of the difference between surf beat forcing and dissipation, but does not allow us to evaluate forcing and dissipation separately. We will use the method developed in section 2 to analyze data collected from a beach near Duck, North Carolina. We describe the field site and instrumentation in section 3 and present results in section 4. We find that net surf beat forcing (or dissipation) was strong when incident waves were large and weak when incident waves were small. Forcing exceeded dissipation outside the surf zone and dissipation exceeded forcing inside the surf zone. During storms, shoreward surf beat propagation maintained surf beat energy inside the saturated surf zone. We discuss the implications of our results and present our conclusions in section 5.

## 2. Energy Equation

[10] Schäffer [1993] derived an energy balance equation for surf beat by assuming that beat frequencies are much lower than incident wave frequencies. In this section we show that a slightly modified form of Schäffer's energy equation applies even when beat frequencies are not much lower than incident wave frequencies. This result is useful because beat frequencies are often not much lower than incident-wave frequencies (surf beat frequencies are as high as 0.05 Hz and the peak frequency of incident waves is often only 0.1 Hz). We also derive a simpler energy equation for a statistically steady wave field on a long, straight beach.

[11] Let  
 $t$  = time,  
 $x_j = j$ 'th horizontal coordinate ( $j = 1$  or  $2$ ),  
 $\mathbf{u}$  = horizontal water velocity,  
 $u_j = j$ 'th component of  $\mathbf{u}$ ,  
 $h$  = still water depth,  
 $\eta$  = sea surface elevation (above still water level),  
 $g$  = gravitational acceleration.  
 Also, for any variable  $X$ , let  $\langle X \rangle_\omega$  be the time-varying complex amplitude of a frequency  $\omega$  Fourier component of  $X$  (see Appendix A1 for definition).

[12] In Appendix A we derive the equation for the time-varying energy of frequency  $\omega$  surf beat

$$\frac{\partial \mathcal{E}(\omega)}{\partial t} + \nabla \cdot \mathbf{w}(\omega) + \mathcal{F}(\omega) + \mathcal{D}(\omega) = 0, \quad (2)$$

where

$$\mathcal{E}(\omega) = h|\langle \tilde{\mathbf{u}} \rangle_\omega|^2 + g|\langle \eta \rangle_\omega|^2, \quad (3)$$

$$\mathbf{w}(\omega) = 2\Re[hg\langle \eta \rangle_\omega \langle \tilde{\mathbf{u}} \rangle_\omega], \quad (4)$$

$$\mathcal{F}(\omega) = 2\Re\left[\langle \tilde{u}_j \rangle_\omega \frac{\partial \langle T_{j,k} \rangle_\omega}{\partial x_k}\right], \quad (5)$$

$\mathcal{D}(\omega)$  = and depth-integrated rate of dissipation at frequency  $\omega$ ,  $\Re$  = real part,

$$\tilde{\mathbf{u}} = \mathbf{u} + \frac{\mathbf{M}}{h}, \quad (6)$$

$$T_{j,k} = \int_{-h}^{\eta} u_j u_k dz + \delta_{j,k} \int_0^{\eta} \frac{p}{\rho} dz, \quad (7)$$

$$\mathbf{M} = \int_0^{\eta} \mathbf{u} dz, \quad (8)$$

$$\delta_{j,k} = \begin{cases} 1 & j = k \\ 0 & j \neq k \end{cases} \quad (9)$$

The summation convention has been used, so repeated indices are summed over all allowable values.

[13] Equation (2) applies to strongly nonlinear waves. However, in a strongly nonlinear wave field, some energy is shared between waves with different frequencies, and the wave energy at a single frequency is not well defined. Consequently, interpretation of equation (2) is difficult unless nonlinear interactions are weak.

[14]  $\bar{\mathbf{u}}$  is the depth-integrated mass transport divided by the still water depth. The momentum flux tensor  $T$  contains contributions from both the mean flow and the wave field. Variations in radiation stress [Longuet-Higgins and Stewart, 1964] are included in  $T$ .  $\mathbf{M}$  is the Stokes drift.

[15]  $\mathcal{E}(\omega)$  is, except for a small Stokes drift contribution, the depth-integrated energy of a wave with frequency  $\omega$ .  $\mathbf{w}(\omega)$  is the the wave energy flux, and represents the depth-integrated rate of working by the water pressure on the water motion.  $\mathcal{F}(\omega)$  is the depth-integrated rate of working by the momentum flux gradient on the water motion.

[16] Nonlinear interactions between waves are associated with the momentum flux  $\langle T_{j,k} \rangle_{\omega}$  and Stokes drift  $\langle \mathbf{M} \rangle_{\omega}$  terms of equation (2). For example, consider the nonlinear component of the wave energy flux,  $g \langle \eta \rangle_{\omega} \langle \mathbf{M} \rangle_{-\omega}$ , in the shallow water limit where  $\langle \mathbf{M} \rangle_{\omega} = \langle \eta \mathbf{u} \rangle_{\omega}$ . From a generalization of Parseval's theorem [e.g., Batchelor, 1960],

$$\langle \eta \mathbf{u} \rangle_{-\omega} = \sum_{\omega_1=-\infty}^{\infty} \langle \eta \rangle_{-\omega-\omega_1} \langle \mathbf{u} \rangle_{\omega_1}, \quad (10)$$

so  $\langle \eta \rangle_{\omega}$ ,  $\langle \eta \rangle_{-\omega-\omega_1}$  and  $\langle \mathbf{u} \rangle_{\omega_1}$  form a triad of nonlinearly interacting waves for every value of  $\omega_1$ .

[17] Equation (2) was derived by assuming that beat frequency pressure fluctuations are hydrostatic (equation (A13)), and by neglecting the depth dependence of beat frequency fluctuations in horizontal velocity (equation (A14)). These assumptions are correct to leading order for Boussinesq surf beat and exact in the shallow water limit. Neglected effects include reductions in water pressure associated with the vertical flux of vertical momentum (which, as we show in Appendix A, probably leads to errors of less than 5%), and nonpotential flow in the bottom boundary layer (which is negligible if boundary layer thickness is small compared to the water depth). Equation (2) is very similar to the energy equation of Schaffer [1993], but does not rely on the assumption that the surf beat period is much longer than the incident wave period.

[18] Let  $x$  and  $y$  be the cross-shore and longshore coordinates respectively ( $x$  positive onshore). Let  $u$  and  $v$  be the  $x$  and  $y$  components of the velocity  $\mathbf{u}$ . Applying the expectation operator  $E[\cdot]$  to equation (2), assuming stationarity ( $\partial E[\cdot]/\partial t = 0$ ) and longshore homogeneity ( $\partial E[\cdot]/\partial y = 0$ ),

and gathering nonlinear terms together into a single term  $-\mathcal{N}(\omega)$  gives

$$\frac{\partial E[q_x(\omega)]}{\partial x} + E[\mathcal{D}(\omega)] - E[\mathcal{N}(\omega)] = 0, \quad (11)$$

where

$$q_x = 2h\Re[g \langle \eta \rangle_{\omega} \langle u \rangle_{-\omega}], \quad (12)$$

$$\mathcal{N}(\omega) = -2\Re \left[ \frac{\partial g \langle \eta \rangle_{\omega} \langle M \rangle_{-\omega}}{\partial x} + \langle \bar{u}_j \rangle_{\omega} \frac{\partial \langle T_{j,k} \rangle_{\omega}}{\partial x_k} \right]. \quad (13)$$

[19] From equation (12)

$$E[q_x(\omega)]/(\Delta\omega) = ghC_{\eta,u}(\omega), \quad (14)$$

where

$$C_{\eta,u}(\omega) = 2\Re(E[\langle \eta \rangle_{\omega} \langle u \rangle_{-\omega}]) / (\Delta\omega) \quad (15)$$

is the density of the cospectrum between  $u$  and  $\eta$  at frequency  $\omega$  ( $\Delta\omega$  is the frequency resolution defined by equation (A2)).

[20] Eldeberky and Battjes [1996], Elgar et al. [1997], Chen and Guza [1997], and Herbers et al. [2000] used equation (11) to study wave shoaling, but they assumed shoreward propagation (although Herbers et al. [2000] allowed for small departures from this assumption), so to leading order

$$q_x(\omega) = \mathcal{E}(\omega)Cg(\omega), \quad (16)$$

where  $Cg(\omega) =$  group velocity. The assumption of shoreward propagation is probably a good approximation for the incident wave frequencies to which equation (16) has primarily been applied, but its application to surf beat is not justified. Reflection of surf beat from the shore, broad directional spread, and refractive trapping of edge waves ensure that equation (16) does not apply to surf beat. In contrast, equation (14) allows for reflection and directional spread and is free from these problems.

[21] Integrating equation (11) from  $x = a$  to  $x = b$  and applying equation (14) gives

$$\begin{aligned} & [hC_{p,u}(\omega)]_{x=b} - [hC_{p,u}(\omega)]_{x=a} \\ & + \int_{x=a}^b (E[\mathcal{D}'(\omega)] - E[\mathcal{N}'(\omega)]) dx = 0, \end{aligned} \quad (17)$$

where  $\mathcal{D}'(\omega) = \mathcal{D}(\omega)/(\omega)$  is the dissipation per unit frequency (similarly for  $\mathcal{N}'(\omega)$ ).

[22] Given measurements of water pressure, water velocity, and mean water depth at two points  $x = a$  and  $x = b$  in the cross-shore, equation (17) can be solved for the excess of dissipation over forcing (negative if forcing exceeds dissipation) between  $a$  and  $b$ . Alternatively, we can choose  $b$  to be the shoreline, across which there is no flux of surf beat energy. Then the shoreward energy flux at  $x = a$  equals

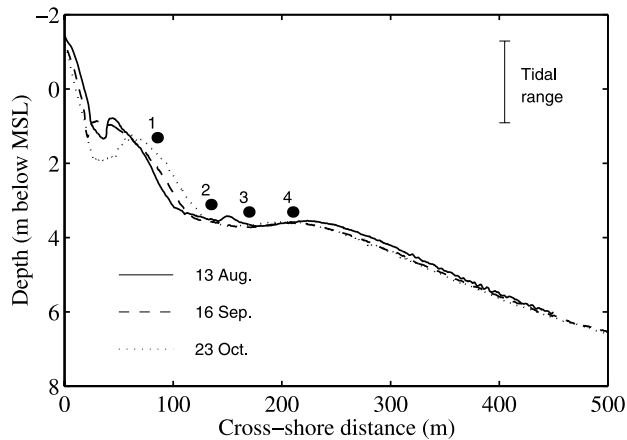


**Figure 1.** Measured beach profiles and location of instrumented frames 1–4.

the excess of dissipation over forcing onshore of  $a$ . Unfortunately, it is difficult to separate the forcing and dissipation terms of equation (17), but the difference between forcing and dissipation still provides useful information. Equation (17) applies at every surf beat frequency, but for simplicity we will integrate equation (17) over all surf beat frequencies to obtain a total surf beat energy balance.

### 3. Field Site and Instrumentation

[23] We will analyze data collected on an ocean beach near Duck, North Carolina by the Dalhousie nearshore research group during the Sandyduck beach experiment of 1997. Figure 1 shows the cross-shore array of four instrumented frames from which the data were collected, together with measured beach profiles. Water pressures and velocities were measured at 2 Hz at every frame. During the Sandyduck experiment, the U.S. Army Corps of Engineers regularly measured seabed elevation profiles using the Coastal Research Amphibious Buggy [Lee and Birkemeier, 1993]. Seabed elevations beneath the instrumented frames were also measured continuously using sonar altimeters.

### 4. Results

[24] Cross-periodograms between water pressure and velocity were calculated from quadratically detrended half-hour time series. Spectra of the wave energy flux were estimated by averaging these cross-periodograms and applying equations (14) and (A13). Figure 2 shows a spectrum of the shoreward energy flux measured over two hours during a storm on day 293. The shaded region of Figure 2 is the surf beat band (0.005–0.05 Hz). For every half hour of the experiment we estimated the total surf beat energy flux  $q_x$  by integrating raw cross-periodograms between pressure and velocity over the entire surf beat band and multiplying by the water depth  $h$ . Other statistics, such as significant wave height and the surf beat sea surface elevation variance, were also calculated every half hour. We estimated sea surface elevations from water pressure measurements using linear wave theory. The significant wave height was calculated as  $4\overline{\eta_w^2}^{1/2}$ , where  $\overline{\eta_w^2}$  is the sea surface elevation variance due to waves with frequencies greater than 0.05 Hz.

[25] Equation (11) neglects the longshore gradient of the longshore energy flux. The ratio of the longshore flux gradient to the cross-shore flux gradient is

$$R = \frac{\left| \frac{\partial q_y / \partial y}{\partial q_x / \partial x} \right| \approx \frac{q_y}{q_x} \frac{L_x}{L_y}, \quad (18)$$

where

$q_y$  = longshore component of surf beat energy flux,

$L_x$  = cross-shore length scale over which  $q_x$  varies,

$L_y$  = longshore length scale over which  $q_y$  varies.

Since the beach at Duck is long and straight, we assume  $L_x/L_y < 1$ . When incident waves were large, the observed mean square longshore surf beat energy flux was usually an order of magnitude smaller than the mean square cross-shore surf beat energy flux. When incident waves were small, the longshore and cross-shore energy fluxes were of the same magnitude. Therefore, when incident waves were large  $R \ll 1$ , so the longshore uniform approximation made in the derivation of equation (11) was reasonable. We cannot be sure how accurate the longshore uniform approximation was when incident waves were small.

[26] Figure 3 shows the time series of significant wave height, surf beat sea surface elevation variance, and shoreward surf beat energy flux, measured at frame 4. Similar results were obtained from the other three frames. Surf beat energy increased with increasing significant wave height, consistent with the findings of Tucker [1950], Holman [1981], Guza and Thornton [1985], and others. The surf beat energy flux was directed onshore in 86% of cases, suggesting that the nearshore zone (<3.5 m depth) was usually a region of net surf beat dissipation during the Sandyduck experiment (equation (17)). Shoreward energy fluxes were most pronounced when incident waves were large: when the significant wave height was greater than 1 m the surf beat energy flux was always directed onshore. The observed shoreward energy flux does not imply that surf beat forcing was weak near the shore, but it does imply that dissipation was usually stronger than forcing. During the Sandyduck experiment, incident wave (0.05–0.33 Hz) energy fluxes ranged from  $0.08 \text{ m}^4 \text{ s}^{-3}$  to  $12 \text{ m}^4 \text{ s}^{-3}$  and were always directed onshore.

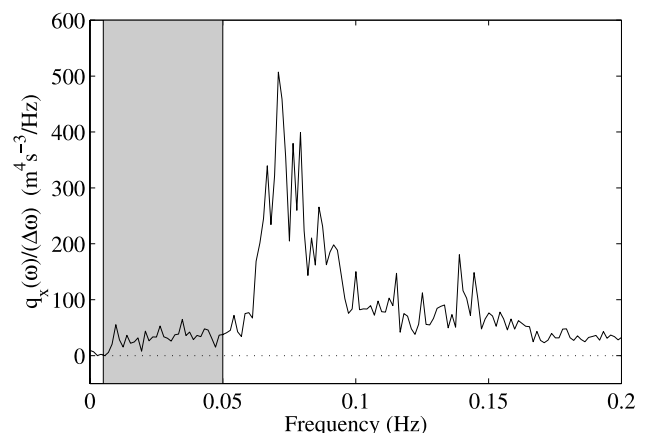


**Figure 2.** Spectrum of the energy flux density  $q_x(\omega)/(\Delta\omega)$  at frame 1 for a two hour period following 10:30 pm on day 293, estimated using equation (14). The shaded region is the surf beat band. The spectral estimates have 10 dof.

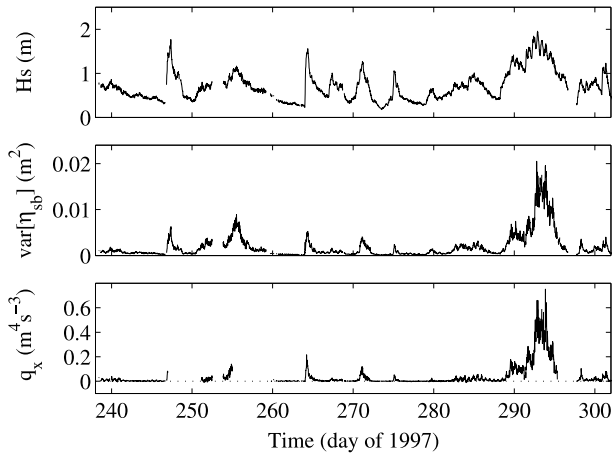


**Figure 3.** Time series of half-hourly significant wave height,  $H_s$ , surf beat sea surface elevation variance,  $\overline{\eta_{sb}^2}$ , and shoreward surf beat energy flux,  $q_x$ , during Sandyduck at frame 4 ( $\approx 3.5$  m depth).

[27] Figure 4 shows the significant wave height  $H_s$  as a function of water depth at frames 1 and 4. Wave heights were limited by breaking, as described by the relation

$$H_s \leq \gamma h, \quad (19)$$

where the breaker ratio  $\gamma$  equals 0.66 at frame 1 and 0.43 at frame 4. *Sallenger and Holman* [1985] and *Raubenheimer et al.* [1996] discuss the application of equation (19) to the surf zone at Duck. In order to determine approximately

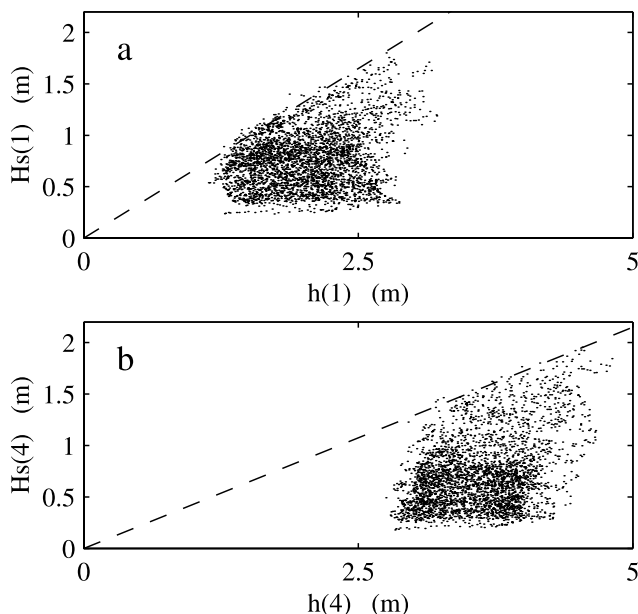


**Figure 4.** Significant wave height,  $H_s$ , versus water depth,  $h$ : (a) frame 1 and (b) frame 4. Dashed line is  $H_s = \gamma h$ , where  $\gamma$  is 0.66 at frame 1 and 0.43 at frame 4. Each data point is estimated from a half-hour time series segment.

whether frame 1 was inside or outside the saturated surf zone, we define the shoaled significant wave height

$$H_s' = [h(4)/h]^{1/4} H_s(4), \quad (20)$$

where  $H_s(4)$  and  $h(4)$  are the significant wave height and water depth at frame 4, and  $h$  is the local water depth.  $H_s'$  is the wave height that would be observed given linear, nondissipative shoaling of shore normal shallow water waves. Roughly, frame 1 is inside (outside) the saturated surf zone when  $H_s'/h$  is greater than (less than)  $\gamma$  at frame 1. At frame 4,  $H_s' = H_s$ .

[28] The shoreward surf beat energy flux shown in Figure 3 implies some shoreward propagation of surf beat. We define the onshore progressiveness  $\rho$  as the ratio between the actual surf beat energy flux, calculated from equation (14), and the surf beat energy flux expected for a purely shore normal, shoreward propagating wave, calculated from equation (16). If all surf beat propagates directly shoreward  $\rho = 1$ , if all surf beat propagates directly seaward  $\rho = -1$ , and if all surf beat is standing in the cross-shore  $\rho = 0$ . Directional spreading of waves (away from shore normal) reduces the magnitude of  $\rho$ . We estimated the total surf beat energy density as twice the potential energy density, or

$$\mathcal{E} = g \overline{\eta_{sb}^2}, \quad (21)$$

where  $\overline{\eta_{sb}^2}$  is the sea surface elevation variance due to surf beat. The use of equation (20) introduced small errors into our  $\mathcal{E}$  estimates, but allowed us to separate surf beat (gravity wave) energy from the shear wave energy that often contributes a large proportion of the total low-frequency kinetic energy [*Lippmann, 1999*]. Figure 5 shows the

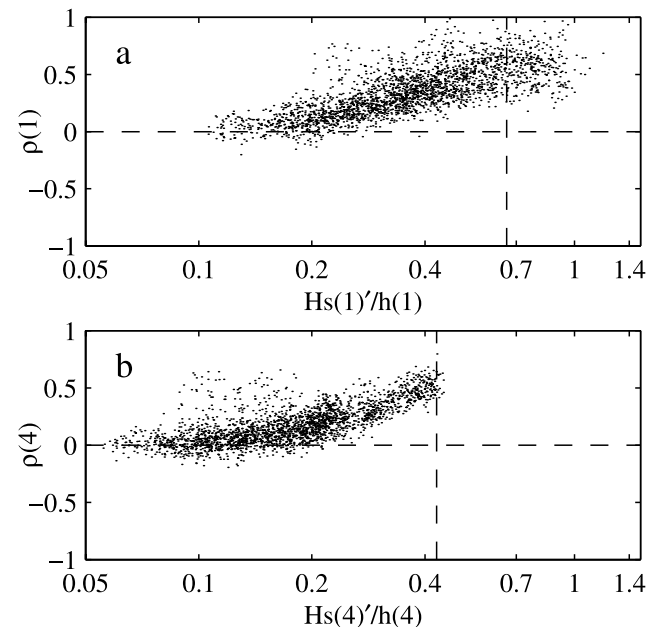


**Figure 5.** Onshore progressiveness of surf beat,  $\rho = q_x/\mathcal{E}Cg$ , versus shoaled significant wave height (equation (20)) divided by water depth,  $H_s'/h$ : (a) frame 1 and (b) frame 4. The vertical dashed lines indicate  $H_s'/h = \gamma$ . Each data point is estimated from a half-hour time series segment.

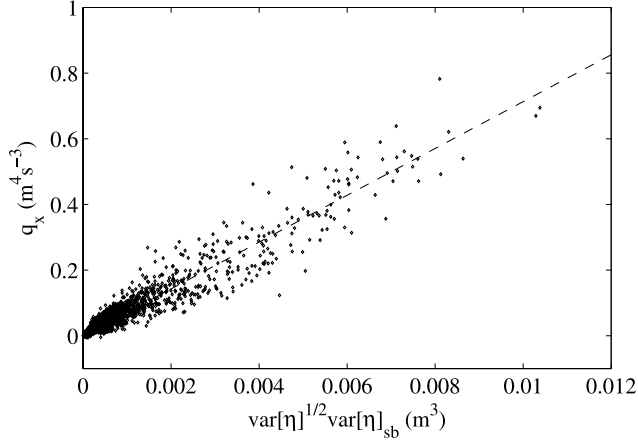


**Figure 6.** Onshore surf beat energy flux,  $q_x$ , versus  $\overline{\eta^2}^{1/2} \overline{\eta}_{sb}^2$  at frame 1. Dashed line is  $q_x = \beta \overline{\eta^2}^{1/2} \overline{\eta}_{sb}^2$ , with  $\beta$  chosen to give least squares fit. Each data point is estimated from a half-hour time series segment.

observed dependence of  $\rho$  on the nondimensional shoaled wave height  $Hs'/h$ . When the nondimensional wave height was small,  $\rho \approx 0$  and surf beat was approximately standing in the cross shore. When the nondimensional wave height was large,  $\rho > 0$  and there was a significant shoreward propagating component of surf beat.

[29] We will now show that the observed net surf beat dissipation can be predicted using a standard bottom stress parameterization. The dissipation of the energy of a frequency  $\omega$  wave by bottom friction is

$$\mathcal{D}(\omega) = f_e |\mathbf{u}| \langle \mathbf{u} \rangle_\omega^2, \quad (22)$$

where  $f_e$  is a dimensionless energy dissipation factor. Values of  $f_e$  observed in the field for incident frequency waves are usually in the range 0.01–1 [Sleath, 1984].

[30] Feddersen *et al.* [1998] showed that the drag force (divided by the water density),  $F$ , retarding the mean longshore current,  $\bar{v}$ , at Duck is

$$F = c_f |\mathbf{u}| \bar{v},$$

where the bottom drag coefficient,  $c_f$ , is roughly 0.001 outside the surf zone and 0.003 inside the surf zone. Applying the same parameterization to surf beat

$$\begin{aligned} \mathbf{F}(\omega) &= c_f |\mathbf{u}| \langle \mathbf{u} \rangle_\omega, \\ \Rightarrow \mathcal{D}(\omega) &= \mathbf{F}(\omega) \cdot \langle \mathbf{u} \rangle_{-\omega} = c_f |\mathbf{u}| \langle \mathbf{u} \rangle_\omega^2. \end{aligned} \quad (23)$$

Equation (22) differs from equation (21) only in the magnitude of the nondimensional coefficient: dissipation factors for waves are one or two orders of magnitude larger than drag coefficients for the mean current [Nielsen, 1992].

[31] From equations (21) and (22) the total dissipation of surf beat energy by bottom drag scales with

$$\frac{\overline{|\mathbf{u}|^2}^{1/2}}{\overline{|\mathbf{u}|_{sb}^2}}, \quad (24)$$

where  $(\overline{|\mathbf{u}|_{sb}^2})$  is the contribution to velocity variance from surf beat frequencies. To separate gravity wave dissipation

from shear wave dissipation we rewrite equation (23) in terms of the sea surface elevation variance. For gravity waves in shallow water [Lippmann *et al.*, 1999]

$$\overline{|\mathbf{u}|^2} \approx g \overline{\eta^2} / h, \Rightarrow \overline{\mathcal{D}(\omega)} \approx f_e (g/h)^{3/2} \overline{\eta^2}^{1/2} \overline{\eta}_{sb}^2. \quad (25)$$

From equations (17) and (24)

$$q_x|_{x=a} \approx \int_{x=a}^{shore} \left( f_e (g/h)^{3/2} \overline{\eta^2}^{1/2} \overline{\eta}_{sb}^2 - E[\mathcal{N}_{sb}] \right) dx. \quad (26)$$

[32] Figure 6 shows that the shoreward surf beat energy flux at frame 1 scales with  $\overline{\eta^2}^{1/2} \overline{\eta}_{sb}^2$  ( $r^2 = 0.92$ ), as predicted by equation (25) if the nonlinear energy exchange to the surf beat band,  $\mathcal{N}_{sb}$ , is neglected. An order of magnitude estimate for  $f_e$  is

$$f_e \approx \frac{\beta}{(g/h)^{3/2} l}, \quad (27)$$

where  $l$  is the distance from frame 1 to the shore,  $\beta$  is the slope of the dashed line in Figure 6, and  $h$  is a typical water depth shoreward of frame 1 (taken to be half the depth at frame 1). Applying equation (26) gives  $f_e \approx 0.08$ , which is a normal value for a wave dissipation factor and is 27–80 times larger than the drag coefficients Feddersen *et al.* [1998] found were appropriate for the mean longshore current.

[33] We neglected  $\mathcal{N}_{sb}$  in the derivation of equation (26). If  $\mathcal{N}_{sb} > 0$  (i.e., if nonlinear interactions force, rather than dissipate, surf beat) then actual rates of dissipation and true  $f_e$  values were higher than we estimated. Alternatively, nonlinear damping ( $\mathcal{N}_{sb} < 0$ , [e.g., Schäffer, 1993; Van Dongeren *et al.*, 1996]) could account for some of the observed energy loss, in which case true  $f_e$  values would be lower than estimated. However, the slope  $\beta$  was largely determined by the strong energy fluxes that were measured during storms, when frame 1 was well inside the saturated surf zone (Figure 4) and nonlinear forcing was probably weak. We also assumed that wave velocity variances were constant onshore of frame 1. This assumption might introduce a significant error into our  $f_e$  estimate. Because of these crude assumptions, our  $f_e$  estimate can only be regarded as an order of magnitude approximation. Furthermore, we cannot be sure that bottom stress was the mechanism responsible for dissipating surf beat, in spite of the good agreement between observed dissipation and the standard bottom stress parameterization. Nevertheless, it is useful to note that net surf beat dissipation in the surf zone can be parameterized in a simple manner.

[34] In section 1 we discussed  $Q$  as a measure of the strength of surf beat dissipation. Since we can measure only spatially averaged net forcing or dissipation, we cannot measure  $Q$  values for individual surf beat modes. Instead, we define the net forcing strength

$$\begin{aligned} S &= \frac{\text{Net surf beat energy generated in one beat period}}{\text{Total surf beat energy}}, \\ &\Rightarrow S = \frac{\int_{x=a}^b (E[\mathcal{N}]) - E[\mathcal{D}] dx}{\omega \int_{x=a}^b \mathcal{E} dx}, \end{aligned} \quad (28)$$

where  $\mathcal{N}$ ,  $\mathcal{D}$ , and  $\mathcal{E}$  are integrated over the surf beat band. From equation (17)

$$S \approx \frac{q_{x|_{x=b}} - q_{x|_{x=a}}}{(0.025\text{Hz}) \int_{x=a}^b \mathcal{E} dx}, \quad (29)$$

where 0.025Hz has been chosen as a typical surf beat frequency. Since this “typical” beat frequency was chosen somewhat arbitrarily, only the sign and order of magnitude of  $S$  are significant. Where possible we estimated the integral in equation (28) using the trapezoidal rule. To estimate the integral between between frame 1 and the shore, we multiplied the energy density at frame 1 by the distance to the shore. The energy density  $\mathcal{E}$  was estimated using equation (20).

[35]  $S$  is positive (negative) if total forcing exceeds total dissipation (dissipation exceeds forcing) between  $x = a$  and  $x = b$ . If  $|S|$  is order one, then the surf beat energy forced (or dissipated) between  $x = a$  and  $x = b$  in a single beat period is of the same order as the total amount of surf beat energy stored between  $x = a$  and  $x = b$ . If  $|S| \ll 1$ , then net forcing (or dissipation) is weak, but this does not imply that actual forcing and dissipation are weak. If strong forcing and strong dissipation happen to cancel, then  $S \ll 1$ . Therefore, large  $|S|$  values indicate strong forcing or dissipation, whereas small  $|S|$  values are ambiguous.

[36] Figure 7a shows the estimated strength of net surf beat forcing,  $S$ , for the region between frames 1 and 4. Figure 7b shows  $S$  for the region between frame 1 and the shore. The vertical dashed lines indicate the nondimensional wave height at which frame 1 is approximately on the edge of the saturated surf zone. When incident waves were small,  $S$  values were scattered around zero. When incident waves were large,  $S$  was order one, so forcing and dissipation were strong. Between frames 1 and 4 (between about 2 and 3.5 m depth), net forcing increased with increasing wave height until it reached a maximum value when frame 1 was slightly outside the saturated surf zone. When frame 1 was inside the saturated surf zone, dissipation sometimes exceeded forcing between frames 1 and 4. Onshore of frame 1, dissipation usually exceeded forcing and net dissipation grew stronger as incident the wave height increased. We suggest that, when incident waves were large, dissipation was strong inside the surf zone and forcing was strong just outside the surf zone.

[37] From equations (1) and (28) it is clear that  $|S|$  is related to  $2\pi/Q$ , but there are important differences between  $S$  and  $Q$ :  $Q$  measures the dissipation of a single wave (mode of motion), whereas  $S$  measures the net forcing or dissipation of all modes in some limited region. Consequently, we cannot use the measured  $S$  values to estimate  $Q$  values for individual surf beat modes. Nevertheless, the negative, order one  $S$  values observed during storms do indicate that the surf beat energy lost within the surf zone in a single beat period was of the same order as the total surf beat energy stored within the surf zone.

## 5. Discussion and Conclusions

[38] A simple energy balance equation relates the energy flux carried by progressive surf beat to net surf beat forcing or dissipation. We used water pressures, velocities, and

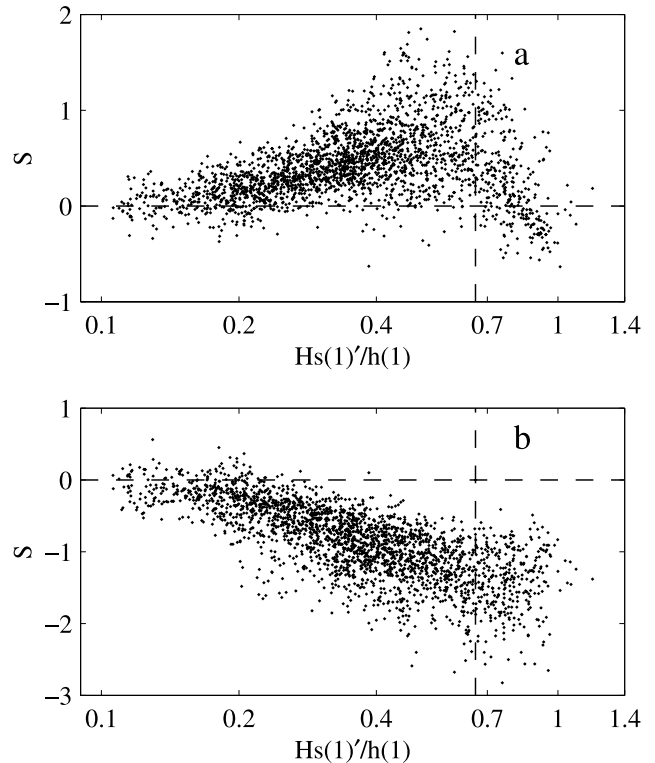


**Figure 7.** Estimated net forcing strength,  $S$ , defined by equation (28) versus shoaled significant wave height (equation (20)) divided by water depth,  $Hs(1)/h$ , at frame 1: (a) net forcing strength between frames 1 and 4 and (b) net forcing strength onshore of frame 1. The vertical dashed lines indicate  $Hs(1)/h(1) = \gamma$ . Each data point is estimated from a half-hour time series segment.

depths measured on a beach near Duck, North Carolina, to estimate cross-shore surf beat energy fluxes, and applied the energy balance equation to estimate net surf beat forcing or dissipation. During the Sandyduck experiment, the near-shore zone ( $<3.5$  m depth) was usually a region of net surf beat dissipation. Shoreward propagating surf beat carried energy into the nearshore zone to balance this net dissipation. This shoreward propagating component of surf beat was large during storms, when the net shoreward energy flux was about half as large as the energy flux that could be carried if all surf beat propagated directly onshore.

[39] The strong shoreward energy fluxes that we observed are consistent with the incomplete reflection of surf beat observed in the surf zone by *Nelson and Gonsalves* [1992], *Raubenheimer et al.* [1995], *Saulter et al.* [1998], *Henderson et al.* [2001], and *Sheremet et al.* [2001].

[40] Most existing surf beat models do not predict the strong shoreward propagation that we observed because they do not simulate strong surf zone dissipation. Unforced, undamped surf beat models [*Eckart*, 1951; *Ursell*, 1952; *Kenyon*, 1970; *Holman and Bowen*, 1979, 1982; *Howd et al.*, 1992; *Bryan and Bowen*, 1996] predict that surf beat has a cross-shore standing structure. Nondissipative and weakly dissipative models that allow for the possibility of edge wave resonance [*Gallagher*, 1971; *Bowen and Guza*, 1978; *Schäffer*, 1994; *Lippmann et al.*, 1997] also predict that surf beat is cross-shore standing. The breakpoint-forcing model

of *Symonds et al.* [1982] predicts cross-shore standing waves onshore of the breakpoint and seaward propagating waves offshore of the breakpoint. The models of *Schäffer* [1993] and *Van Dongeren et al.* [1996] predict that nonlinear forcing due to intermittent wave breaking opposes incident bound wave motions, leading to net nonlinear damping of surf beat at the breakpoint and shoreward propagation just outside the breakpoint. However, these last three models exclude the possibility of edge wave resonance through the arbitrary assumption that forcing is entirely shore normal.

[41] During the Sandyduck experiment, dissipation was strongest well inside the saturated surf zone, exactly where incident waves were limited by breaking and surf beat made an important contribution to the total flow field. We suggest that models of surf beat dynamics should incorporate rapid surf zone dissipation.

[42] A standard bottom dissipation parameterization predicted the observed net surf beat dissipation well. The wave dissipation factor for surf beat was  $O(10^{-1})$ , within the range of dissipation factors usually observed for higher-frequency incident waves.

[43] The region between 2 m and 3.5 m depth was a region of net surf beat forcing, except when incident waves were very large and the saturated surf zone extended beyond 2 m depth. We suggest that surf beat forcing usually exceeded dissipation outside the surf zone, whereas dissipation exceeded forcing inside the surf zone. This is consistent with the cross-shore structure of surf beat forcing predicted by *Longuet-Higgins and Stewart* [1962] and *Symonds et al.* [1982] and with the suggestion of *Guza and Bowen* [1976a] and others that surf beat dissipation might be most rapid inside the surf zone.

[44] Surf beat forcing and dissipation were very strong during storms. When incident waves were large, the surf beat energy dissipated within the surf zone during a single beat period was of the same order as the total surf beat energy stored within the surf zone. The surf beat energy forced in a single beat period near the edge of the surf zone was also of the same order as the total surf beat energy stored near the edge of the surf zone.

## Appendix A: Derivation of Nonlinear Frequency Domain Energy Equation

### A1. Fourier Representation of a Time-Varying Wave Field

[45] A time series  $X(t)$  can be represented by the progressive Fourier series

$$X(t) = \sum_{j=-\infty}^{\infty} e^{i(j\Delta\omega)t} \langle X \rangle_{j\Delta\omega}, \quad (\text{A1})$$

where

$$\Delta\omega = 2\pi/L \quad (\text{A2})$$

is the frequency resolution, and

$$\langle X \rangle_{\omega} = \frac{1}{L} \int_{t'=-L/2}^{t'+L/2} e^{-i\omega t'} X(t') dt' \quad (\text{A3})$$

is the complex amplitude of a frequency- $\omega$  sinusoid fitted to a length  $L$  segment of  $X$  centered on time  $t$ . Note that  $\langle X \rangle_{\omega}$  is a function of time  $t$ .

[46] We now derive an identity for use in section A3. From equation (A1),

$$\frac{\partial X}{\partial t} = \frac{\partial}{\partial t} \sum_{j=-\infty}^{\infty} e^{i(j\Delta\omega)t} \langle X \rangle_{j\Delta\omega}, \quad (\text{A4})$$

so

$$\frac{\partial X}{\partial t} = \sum_{j=-\infty}^{\infty} e^{i(j\Delta\omega)t} \left[ i(j\Delta\omega) \langle X \rangle_{j\Delta\omega} + \frac{\partial \langle X \rangle_{j\Delta\omega}}{\partial t} \right]. \quad (\text{A5})$$

But, by definition,

$$\frac{\partial X}{\partial t} = \sum_{j=-\infty}^{\infty} e^{i(j\Delta\omega)t} \left\langle \frac{\partial X}{\partial t} \right\rangle_{j\Delta\omega}, \quad (\text{A6})$$

so, from equations (A5) and (A6)

$$\left\langle \frac{\partial X}{\partial t} \right\rangle_{\omega} = i\omega \langle X \rangle_{\omega} + \frac{\partial \langle X \rangle_{\omega}}{\partial t}. \quad (\text{A7})$$

Now

$$\frac{\partial \langle X \rangle_{\omega} \langle X \rangle_{-\omega}}{\partial t} = \langle X \rangle_{\omega} \frac{\partial \langle X \rangle_{-\omega}}{\partial t} + \langle X \rangle_{-\omega} \frac{\partial \langle X \rangle_{\omega}}{\partial t}. \quad (\text{A8})$$

Combining equations (A7) and (A8), and noting that  $\langle X \rangle_{-\omega}$  is the complex conjugate of  $\langle X \rangle_{\omega}$  for any real  $X$ , gives

$$\frac{\partial |\langle X \rangle_{\omega}|^2}{\partial t} = 2\Re \left[ \langle X \rangle_{\omega} \left\langle \frac{\partial X}{\partial t} \right\rangle_{-\omega} \right]. \quad (\text{A9})$$

### A2. Mass and Momentum Conservation

[47] An exact, depth-integrated momentum equation for waves in water of constant density and arbitrary depth is [*Phillips*, 1977, equation (3.6.7)]

$$\frac{\partial}{\partial t} \int_{-h}^{\eta} u_j dz + \frac{\partial}{\partial x_k} \int_{-h}^{\eta} u_j u_k dz + \frac{\partial}{\partial x_j} \int_{-h}^{\eta} \frac{p}{\rho} dz - \frac{p}{\rho} \frac{\partial h}{\partial x_j} = 0, \quad (\text{A10})$$

$$\Rightarrow \int_{-h}^0 \frac{\partial u_j}{\partial t} dz + \int_{-h}^0 \frac{\partial (p/\rho)}{\partial x_j} dz + \frac{\partial T_{j,k}}{\partial x_k} + \frac{\partial M_j}{\partial t} = 0, \quad (\text{A11})$$

where  $T$  and  $M$  are defined by equations (7) and (8),  $p$  = water pressure, and  $\rho$  = water density.

[48] Equation (A11) can be rewritten using the Fourier components defined by equations (7) and (8):

$$\int_{-h}^0 \left\langle \frac{\partial u_j}{\partial t} \right\rangle_{\omega} dz + \frac{1}{\rho} \frac{\partial \langle p \rangle_{\omega}}{\partial x_j} dz + \frac{\partial \langle T_{j,k} \rangle_{\omega}}{\partial x_k} + \left\langle \frac{\partial M_j}{\partial t} \right\rangle_{\omega} = 0. \quad (\text{A12})$$



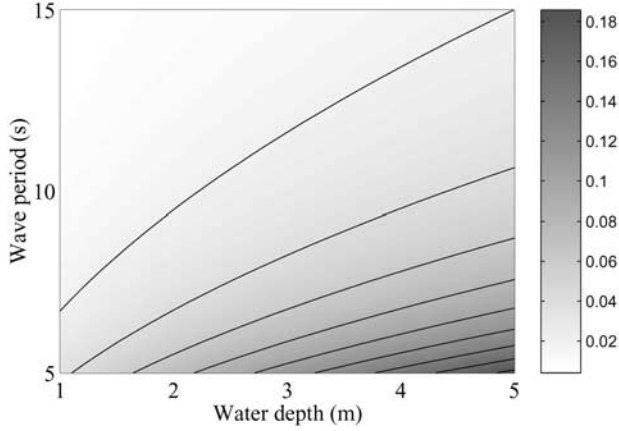


**Figure A1.** Effect of water depth and wave period on the ratio  $\mu$  between neglected and retained radiation stress components. Interval between contours is 0.02. Lowest contour is  $\mu = 0.02$ .

We now approximate the motion at frequency  $\omega$  by assuming

$$\langle p \rangle_\omega = \rho g \langle \eta \rangle_\omega, \quad (\text{A13})$$

$$\langle u_j \rangle_\omega \text{ is independent of } z. \quad (\text{A14})$$

Equations (A13) and (A14) are correct to leading order if frequency  $\omega$  waves satisfy the Boussinesq assumptions, and are exact in the shallow water limit.

[49] In reality,  $\langle p \rangle_\omega$  depends in part on fluxes of vertical momentum. The effects of these momentum fluxes are usually incorporated into the radiation stress, but have been neglected in equation (A13). *Longuet-Higgins and Stewart* [1964] divided the normal radiation stress  $S_{x,x}$  into three components,  $S_{x,x}^{(1)}$ ,  $S_{x,x}^{(2)}$ , and  $S_{x,x}^{(3)}$  [*Longuet-Higgins and Stewart*, 1964, equation (9)]. We have included  $S_{x,x}^{(1)}$  and  $S_{x,x}^{(3)}$  in  $T_{x,x}$  but, through equation (A13), have neglected the pressure deficit term  $S_{x,x}^{(2)}$ . From linear theory, the ratio between the neglected and retained radiation stress terms for long wave groups is

$$\mu \equiv \left| \frac{S_{x,x}^{(2)}}{S_{x,x}^{(1)} + S_{x,x}^{(3)}} \right| = \frac{1 - 2kh / \sinh(2kh)}{2 + 2kh / \sinh(2kh)} \quad (\text{A15})$$

where  $k$  is the wavenumber. Figure A1 shows how  $\mu$  varies with wave period and water depth. During Sandyduck, peak periods were usually about 7–13 s, and depths at the instrumented frames ranged from 1 m to 5 m. From Figure A1, assumption (A13) leads to errors of about 2–5% in radiation stress estimates. Usually  $h|\langle p \rangle_\omega| > |\langle S_{x,x} \rangle_\omega|$ , so the relative error in  $|\langle p \rangle_\omega|$  estimates due to the neglected pressure deficit term was probably less than 5%.

[50] Equation (A14) neglects variations of  $\langle u_j \rangle_\omega$  in the surface and bottom boundary layers. We assume that the thickness of these boundary layers is much less than the water depth, so that the proportion of the depth-integrated momentum stored in the boundary layers is negligible.

[51] From equations (6), (A12), (A13), and (A14),

$$h \left\langle \frac{\partial \tilde{u}_j}{\partial t} \right\rangle_\omega + gh \frac{\partial \langle \eta \rangle_\omega}{\partial x_j} + \frac{\partial \langle T_{j,k} \rangle_\omega}{\partial x_k} = 0. \quad (\text{A16})$$

Similarly, the exact depth-integrated mass conservation equation

$$\frac{\partial \eta}{\partial t} + \frac{\partial}{\partial x_k} \int_{-h}^{\eta} u_k dz = 0, \quad (\text{A17})$$

together with equation (A14), leads to

$$\left\langle \frac{\partial \eta}{\partial t} \right\rangle_\omega + \frac{\partial h \langle \tilde{u}_k \rangle_\omega}{\partial x_k} = 0. \quad (\text{A18})$$

### A3. Energy Equation

[52] Adding  $\langle \tilde{u}_j \rangle_{-\omega} \times$  equation (A16) to the complex conjugate of  $\langle \tilde{u}_j \rangle_{-\omega} \times$  equation (A16) and applying equation (A9) gives

$$\frac{\partial h |\langle \tilde{\mathbf{u}} \rangle_\omega|^2}{\partial t} + 2\Re \left[ gh \langle \tilde{u}_j \rangle_{-\omega} \frac{\partial \langle \eta \rangle_\omega}{\partial x_j} + \langle \tilde{u}_j \rangle_{-\omega} \frac{\partial \langle T_{j,k} \rangle_\omega}{\partial x_k} \right] = 0. \quad (\text{A19})$$

But

$$gh \langle \tilde{u}_j \rangle_\omega \frac{\partial \langle \eta \rangle_\omega}{\partial x_j} = \frac{\partial gh \langle \tilde{u}_j \rangle_{-\omega} \langle \eta \rangle_\omega}{\partial x_j} - g \langle \eta \rangle_\omega \frac{\partial h \langle \tilde{u}_j \rangle_{-\omega}}{\partial x_j}, \quad (\text{A20})$$

so from equations (A18), (A20), and (A9),

$$2\Re \left[ gh \langle \tilde{u}_j \rangle_{-\omega} \frac{\partial \langle \eta \rangle_\omega}{\partial x_j} \right] = 2\Re \left[ \frac{\partial hg \langle \eta \rangle_\omega \langle \tilde{u}_j \rangle_{-\omega}}{\partial x_j} \right] + \frac{\partial g |\langle \eta \rangle_\omega|^2}{\partial t}. \quad (\text{A21})$$

Substituting equation (A21) into equation (A19) gives

$$\frac{\partial \mathcal{E}}{\partial t} + \frac{\partial w_j}{\partial x_j} + \mathcal{F} = 0, \quad (\text{A22})$$

where  $\mathcal{E}$ ,  $w_j$ , and  $\mathcal{F}$  are defined by equations (3)–(5). Finally, adding to equation (A22) a term  $\mathcal{D}$  to represent the effects of dissipation gives equation (2).

[53] **Acknowledgments.** This research was supported by the Izaak Walton Killam Foundation, the Andrew Mellon Foundation, and the Natural Sciences and Engineering Research Council of Canada. Throughout the Sandyduck Experiment, excellent logistical support was provided by the staff of the Field Research Facility of the U.S. Army Engineer Waterways Experiment Station's Coastal Engineering Research Center.

### References

- Batchelor, G., *The Theory of Homogeneous Turbulence*, Cambridge Univ. Press, New York, 1960.  
 Bowen, A., Wave-wave interactions near the shore, *Lect. Notes Phys.*, 64, 102–113, 1977.  
 Bowen, A., and R. Guza, Edge waves and surf beat, *J. Geophys. Res.*, 83, 1913–1920, 1978.  
 Bryan, K., and A. Bowen, Edge wave trapping and amplification on barred beaches, *J. Geophys. Res.*, 101, 6543–6552, 1996.

- Bryan, K., P. Howd, and A. Bowen, Field observations of bar-trapped edge waves, *J. Geophys. Res.*, *103*, 1285–1305, 1998.
- Chen, Y., and R. Guza, Modeling spectra of breaking surface waves in shallow water, *J. Geophys. Res.*, *102*, 25,035–25,046, 1997.
- Chen, Y., and R. Guza, Resonant scattering of edge waves on longshore periodic topography: Finite beach slope, *J. Fluid Mech.*, *387*, 255–269, 1999.
- Eckart, C., Surface waves in water of variable depth, *Wave Rep.* *100*, Scripps Inst. of Oceanogr., La Jolla, Calif., 1951.
- Eldeberky, Y., and J. Battjes, Spectral modeling of wave breaking: Applications of Boussinesq equations, *J. Geophys. Res.*, *101*, 1253–1264, 1996.
- Elgar, S., T. Herbers, M. Okihiro, J. Oltman-Shay, and R. Guza, Observations of infragravity waves, *J. Geophys. Res.*, *97*, 15,573–15,577, 1992.
- Elgar, S., T. Herbers, and R. Guza, Reflection of ocean surface gravity waves from a natural beach, *J. Phys. Oceanogr.*, *24*, 1503–1511, 1994.
- Elgar, S., R. Guza, B. Raubenheimer, T. Herbers, and E. L. Gallagher, Spectral evolution of shoaling and breaking waves on a barred beach, *J. Geophys. Res.*, *102*, 15,797–15,805, 1997.
- Fedderson, F., R. Guza, S. Elgar, and T. Herbers, Alongshore momentum balances in the nearshore, *J. Geophys. Res.*, *103*, 15,667–15,676, 1998.
- Foda, M., and C. Mei, Nonlinear excitation of long-trapped waves by a group of short swells, *J. Fluid Mech.*, *111*, 319–345, 1981.
- Gallagher, B., Generation of surf beat by non-linear wave interactions, *J. Fluid Mech.*, *49*, 1–20, 1971.
- Green, E. I., The story of Q, *Am. Sci.*, *43*, 584–594, 1955.
- Guza, R., and A. Bowen, Resonant interactions for waves breaking on a beach, paper presented at 15th International Conference on Coastal Engineering, Am. Soc. of Civ. Eng., Honolulu, Hawaii, 1976a.
- Guza, R., and A. Bowen, Finite amplitude edge waves, *J. Mar. Res.*, *34*, 269–293, 1976b.
- Guza, R., and R. Davis, Excitation of edge waves by waves incident on a beach, *J. Geophys. Res.*, *79*, 1285–1291, 1974.
- Guza, R., and E. B. Thornton, Swash oscillations on a natural beach, *J. Geophys. Res.*, *87*, 483–491, 1982.
- Guza, R., and E. Thornton, Observations of surf beat, *J. Geophys. Res.*, *90*, 3161–3172, 1985.
- Guza, R., E. Thornton, and R. Holman, Swash on steep and shallow beaches, paper presented at 19th International Conference on Coastal Engineering, Am. Soc. of Civ. Eng., Houston, Tex., 1984.
- Hasselmann, K., W. Munk, and G. MacDonald, Bispectra of ocean waves, in *Proceedings of the Symposium on Time Series Analysis*, edited by M. Rosenblatt, pp. 125–139, John Wiley, New York, 1963.
- Henderson, S. M., S. Elgar, and A. Bowen, Observations of surf beat propagation and energetics, paper presented at 27th International Conference on Coastal Engineering, Am. Soc. of Civ. Eng., Sydney, Australia, 2001.
- Herbers, T., S. Elgar, and R. Guza, Infragravity-frequency (0.005–0.05Hz) motions on the shelf, part 1, Forced waves, *J. Phys. Oceanogr.*, *24*, 917–927, 1994.
- Herbers, T., S. Elgar, and R. Guza, Generation and propagation of infragravity waves, *J. Geophys. Res.*, *100*, 24,863–24,872, 1995a.
- Herbers, T., S. Elgar, R. Guza, and W. O'Reilly, Infragravity-frequency (0.005–0.05Hz) motions on the shelf, part 2, Free waves, *J. Phys. Oceanogr.*, *25*, 1063–1079, 1995b.
- Herbers, T., N. Russnogle, and S. Elgar, Spectral energy balance of breaking waves within the surf zone, *J. Phys. Oceanogr.*, *30*, 2723–2737, 2000.
- Holland, K., B. Raubenheimer, R. Guza, and R. Holman, Runup kinematics on a natural beach, *J. Geophys. Res.*, *100*, 4985–4993, 1995.
- Holman, R., Infragravity energy in the surf zone, *J. Geophys. Res.*, *86*, 6442–6450, 1981.
- Holman, R., and A. Bowen, Edge waves on complex beach profiles, *J. Geophys. Res.*, *84*, 6339–6346, 1979.
- Holman, R., and A. Bowen, Bars, bumps and holes: Models for the generation of complex beach topography, *J. Geophys. Res.*, *87*, 457–468, 1982.
- Holman, R., and A. Bowen, Longshore structure of infragravity wave motions, *J. Geophys. Res.*, *89*, 6446–6452, 1984.
- Howd, P. A., A. Bowen, and R. A. Holman, Edge waves in the presence of strong longshore currents, *J. Geophys. Res.*, *97*, 11,357–11,371, 1992.
- Huntley, D., Long period waves on a natural beach, *J. Geophys. Res.*, *81*, 6441–6449, 1976.
- Huntley, D. A. and C. S. Kim, Is surf beat forced or free?, paper presented at 19th International Conference on Coastal Engineering, Am. Soc. of Civ. Eng., Houston, Tex., 1984.
- Huntley, D., R. Guza, and E. Thornton, Field observations of surf beat, 1, Progressive edge waves, *J. Geophys. Res.*, *86*, 6451–6466, 1981.
- Kenyon, K., A note on conservative edge wave interactions, *Deep Sea Res.*, *17*, 197–201, 1970.
- Lee, G. and W. Birkemeier, Beach and nearshore survey data: 1985–1991, CERC field research facility, *Tech. Rep. CERC-93-3*, U. S. Army Corps of Eng., Vicksburg, Miss., 1993.
- Lippmann, T., R. Holman, and A. Bowen, Generation of edge waves in shallow water, *J. Geophys. Res.*, *102*, 8663–8679, 1997.
- Lippmann, T., T. Herbers, and E. Thornton, Gravity and shear wave contributions to nearshore infragravity wave motions, *J. Phys. Oceanogr.*, *29*, 231–239, 1999.
- List, J., Wave groupiness as a source of nearshore long waves, paper presented at 20th International Conference on Coastal Engineering, Am. Soc. of Civ. Eng., Taipei, Taiwan, 1986.
- List, J., A model for the generation of two-dimensional surf beat, *J. Geophys. Res.*, *97*, 5623–5635, 1992.
- Liu, P. L., A note on long waves induced by short-wave groups over a shelf, *J. Fluid Mech.*, *205*, 163–170, 1989.
- Longuet-Higgins, M., and R. Stewart, Radiation stress and mass transport in gravity waves, with application to “surf beats”, *J. Fluid Mech.*, *13*, 481–504, 1962.
- Longuet-Higgins, M., and R. Stewart, Radiation stresses in water waves: A physical discussion, with applications, *Deep Sea Research*, *11*, 529–562, 1964.
- Masselink, G., Group bound long waves as a source of infragravity energy in the surf zone, *Cont. Shelf Res.*, *15*, 1525–1547, 1995.
- Mathew, J., and T. Akylas, On the radiation damping of finite amplitude edge waves, *Proc. R. Soc. London, Ser. A*, *431*, 419–431, 1990.
- Mei, C. C., and C. Benmoussa, Long waves induced by short-wave groups over an uneven bottom, *J. Fluid Mech.*, *139*, 219–235, 1984.
- Munk, W., Surf beats, *Eos Trans. AGU*, *30*, 849–854, 1949.
- Munk, W., F. Snodgrass, and F. Gilbert, Long waves on the continental shelf: An experiment to separate leaky and trapped waves, *J. Fluid Mech.*, *20*, 529–554, 1964.
- Nelson, R., and J. Gonsalves, Surf zone transformation of wave height to water depth ratios, *Coastal Eng.*, *17*, 49–70, 1992.
- Nielsen, P., *Coastal Bottom Boundary Layers and Sediment Transport*, World Sci., River Edge, N. J., 1992.
- Okihiro, M., R. Guza, and R. Seymour, Bound infragravity waves, *J. Geophys. Res.*, *97*, 11,453–11,469, 1992.
- Oltman-Shay, J., and R. Guza, Infragravity edge wave observations on two California beaches, *J. Phys. Oceanogr.*, *17*, 644–663, 1987.
- Phillips, O., *The Dynamics of the Upper Ocean*, 2nd ed., Cambridge Univ. Press, New York, 1977.
- Raubenheimer, B., R. Guza, S. Elgar, and N. Kobayashi, Swash on a gently sloping beach, *J. Geophys. Res.*, *100*, 8751–8760, 1995.
- Raubenheimer, B., R. Guza, and S. Elgar, Wave transformation across the inner surf zone, *J. Geophys. Res.*, *101*, 25,589–25,597, 1996.
- Ruessink, B., Bound and free infragravity waves in the nearshore zone under breaking and nonbreaking conditions, *J. Geophys. Res.*, *103*, 12,795–12,805, 1998a.
- Ruessink, B., The temporal and spatial variability of infragravity energy in a barred nearshore zone, *Cont. Shelf Res.*, *18*, 585–605, 1998b.
- Sallenger, A. H., and R. A. Holman, Wave energy saturation on a natural beach of variable slope, *J. Geophys. Res.*, *90*, 11,939–11,944, 1985.
- Saulter, A. N., T. J. O'Hare, and P. E. Russell, Analysis of infragravity wave-driven sediment transport on macrotidal beaches, in *Coastal Dynamics*, pp. 1033–1042, Am. Soc. of Civ. Eng., Reston, Va., 1998.
- Schäffer, H., Infragravity waves induced by short-wave groups, *J. Fluid Mech.*, *247*, 551–588, 1993.
- Schäffer, H., Edge waves forced by short-wave groups, *J. Fluid Mech.*, *259*, 125–148, 1994.
- Sheremet, A., R. Guza, S. Elgar, and T. Herbers, Estimating infragravity wave properties from pressure-current meter array observations, paper presented at 27th International Conference on Coastal Engineering, Am. Soc. of Civ. Eng., Sydney, Australia, 2001.
- Sleath, J., *Sea Bed Mechanics*, John Wiley, New York, 1984.
- Symonds, G., D. Huntley, and A. Bowen, Two-dimensional surf beat: Long wave generation by a time-varying breakpoint, *J. Geophys. Res.*, *87*, 492–498, 1982.
- Tucker, M., Surf beats: Sea waves of 1 to 5 min. period, *Proc. R. Soc. London, Ser. A*, *202*, 565–573, 1950.
- Ursell, F., Edge waves on a sloping beach, *Proc. R. Soc., Ser. A*, *214*, 79–97, 1952.
- Van Dongeren, A., I. Svendsen, and F. Sancho, Generation of infragravity waves, paper presented at 25th International Conference on Coastal Engineering, Am. Soc. of Civ. Eng., Orlando, Fla., 1996.